Acta Neuropathol (2011) 121:737–751
DOI 10.1007/s00401-011-0807-1

ORIGINAL PAPER

The optic nerve head is the site of axonal transport disruption, axonal cytoskeleton damage and putative axonal regeneration failure in a rat model of glaucoma

Glyn Chidlow · Andreas Ebneter · John P. M. Wood · Robert J. Casson

Received: 17 November 2010 / Revised: 27 January 2011 / Accepted: 29 January 2011 / Published online: 11 February 2011

Abstract The neurodegenerative disease glaucoma is characterised by the progressive death of retinal ganglion cells (RGCs) and structural damage to the optic nerve (ON). New insights have been gained into the pathogenesis of glaucoma through the use of rodent models; however, a coherent picture of the early pathology remains elusive. Here, we use a validated, experimentally induced rat glaucoma model to address fundamental issues relating to the spatio-temporal pattern of RGC injury. The earliest indication of RGC damage was accumulation of proteins, transported by orthograde fast axonal transport within axons in the optic nerve head (ONH), which occurred as soon as 8 h after induction of glaucoma and was maximal by 24 h. Axonal cytoskeletal abnormalities were first observed in the ONH at 24 h. In contrast to the ONH, no axonal cytoskeletal damage was detected in the entire myelinated ON and tract until 3 days, with progressively greater damage at later time points. Likewise, down-regulation of RGC-specific mRNAs, which are sensitive indicators of RGC viability, occurred subsequent to axonal changes at the ONH and later than in retinas subjected to NMDA-induced somatic excitotoxicity. After 1 week, surviving, but injured, RGCs had initiated a regenerative-like response, as delineated by Gap43 immunolabelling, in a response similar to that seen after ON crush. The data presented here provide robust support for the hypothesis that the ONH is the pivotal site of RGC injury following moderate elevation of IOP, with the resulting anterograde degeneration of axons and retrograde injury and death of somas.

Keywords Glaucoma · Retinal ganglion cell · Optic nerve head · Axonal transport · Axon degeneration · Amyloid precursor protein

Introduction

Glaucoma refers to a family of ocular diseases with multifactorial aetiology united by a clinically characteristic optic neuropathy. Pathologically, glaucoma is characterised by a loss of all retinal ganglion cell (RGC) compartments: somata, axons and dendrites; clinically, loss of axons at the optic nerve head (ONH) heralds the diagnosis of glaucoma. This observation, together with other converging clinical evidence, has given rise to a long-standing belief that the foremost site of injury is at the ONH [39]. Yet, the pathogenesis of glaucoma remains poorly understood. Evidence supporting the ONH as the primary locus of injury is circumstantial, whilst not much is known about the molecular pathways involved in the loss of RGCs and their axons. To date, treatment options for glaucoma remain limited to lowering intraocular pressure (IOP), the highest profile risk factor for the disease [23].

To facilitate a greater understanding of glaucoma, a number of rodent paradigms have been developed. These can broadly be divided into rat models, in which elevated IOP is induced experimentally [33], and mouse models,

Electronic supplementary material The online version of this article (doi:10.1007/s00401-011-0807-1) contains supplementary material, which is available to authorized users.

G. Chidlow (✉) · A. Ebneter · J. P. M. Wood · R. J. Casson
Ophthalmic Research Laboratories, South Australian Institute of Ophthalmology, Hanson Institute Centre for Neurological Diseases, Frome Rd, Adelaide, SA 5000, Australia
e-mail: glyn.chidlow@health.sa.gov.au

G. Chidlow · A. Ebneter · J. P. M. Wood · R. J. Casson
Department of Ophthalmology and Visual Sciences, University of Adelaide, Frome Rd, Adelaide, SA 5000, Australia

where IOP elevation occurs spontaneously [18]. Of particular importance has been the discovery and characterisation of the DBA/2J inbred mouse strain [19]. DBA/2J mice exhibit a form of pigmentary glaucoma featuring an age-related elevation of IOP and progressive optic neuropathy. In recent years, a substantive body of work has been conducted on DBA/2J mice, providing new insights into the spatio-temporal pattern of RGC dysfunction and degeneration. A consistent view on the chronology of pathological events in this disease model is, however, still to be reached. For example, Howell et al. [16] provided robust evidence for an early insult at the lamina of the ONH with Wallerian-like degeneration of axons distal to the site of injury. In contrast, Crish et al. [12] ascertained that axonal transport dysfunction and axon degeneration appear first at the superior colliculus with a distal-proximal progression, findings in broad agreement with earlier work [44]. Furthermore, somatic alterations in RGCs, including downregulation of mRNA synthesis and abnormal neurofilament labelling, have been described as occurring more or less simultaneously [17], or subsequent to [5], retrograde axon transport dysfunction.

Certain strengths of the DBA/2J mouse as a relevant model for human glaucoma, including its gradual progression, unpredictable timing and inter-individual variability, make unequivocal identification of the sequence of events problematic. Here, we use a validated, experimentally induced rat glaucoma model [26] to address several fundamental issues. These include ascertaining the spatio-temporal pattern of orthograde axonal transport disruption and its correlation with IOP elevation, delineating the site of initial axonal cytoskeletal damage and determining any association with altered neurofilament phosphorylation, documenting the timing of RGC somal injury and whether RGCs attempt to regenerate their injured axons, and finally, comparing the pattern of injury observed in glaucoma with those seen after optic nerve crush or NMDA-induced excitotoxicity, the classical methods of eliciting axonal and somato-dendritic death of RGCs, respectively.

Materials and methods

Animals and procedures

This study was approved by the Animal Ethics Committees of the Institute of Medical and Veterinary Science and the University of Adelaide and conforms to the Australian Code of Practice for the Care and Use of Animals for Scientific Purposes, 2004. All experiments conformed to the ARVO Statement for the Use of Animals in Ophthalmic and Vision Research. Adult Sprague–Dawley rats (200–250 g) were housed in a temperature- and humidity-controlled environment with a 12-h light, 12-h dark cycle and were provided with food and water ad libitum.

For experimental glaucoma experiments, rats were anaesthetised with 100 mg/kg ketamine and 10 mg/kg xylazine. Ocular hypertension was then induced in the right eye of each animal by laser photocoagulation of the trabecular meshwork using a slightly modified protocol [14] of the method described by Levkovitch–Verbin et al. [26]. IOPs were measured in both eyes at baseline, 8 h, days 1, 3, 7 and 14 using a rebound tonometer factory calibrated for use in rats. No animals were excluded for reasons relating to inadequate IOP elevation. Two animals were excluded as a result of death under anaesthesia and two due to hyphema. Two cohorts of rats were used in the current study. The first cohort was used for immunohistochemistry/histology of the retina, ONH, optic nerve (ON) and optic tract (OT). The number of rats analysed at each time point was as follows: 8 h ($n = 4$), 1 day ($n = 8$), 3 days ($n = 10$), 7 day ($n = 9$), 14 days ($n = 10$). In addition, three rats were killed at 2 days and used for transverse sectioning of the ONH. For axonal tracing, 4 rats were injected intravitreally with 5 µl of 0.1% AlexaFluor 594-conjugated cholera toxin β-subunit (CTB) dissolved in sterile PBS. After 24 h, right eyes were lasered as above. Rats were killed at 2 days and taken for immunohistochemistry. The second cohort was used for RT-PCR/Western blotting of the retina and ON. The number of rats analysed at each time point was as follows: 1 day ($n = 4$), 3 days ($n = 7$), 7 days ($n = 7$), 14 days ($n = 4$). The chiasm from each rat was taken for immunohistochemistry to verify that the procedure had induced an injury response commensurate with the first cohort.

For excitotoxicity experiments, an intravitreal injection of 30 nmol of NMDA (5 µl in sterile saline) was performed in one eye. The control eye was injected with vehicle. The number of rats analysed at each time point for RT-PCR of the retina was as follows: 6 h ($n = 7$), 1 day ($n = 6$), 3 days ($n = 6$), 7 days ($n = 7$). In addition, four rats were taken at each time point for immunohistochemistry. For ON crush experiments, the superior muscle complex was divided and the ON exposed by blunt dissection. The ON was then crushed 3-mm posterior to the globe under direct visualisation using number 5 forceps for 20 s. ON crush produces complete disruption of the RGC axons, which can be seen as a separation of the proximal and distal optic nerve ends within the meningeal sheath. To avoid confusing retinal ischaemic changes with the effects of crush, the fundus was observed ophthalmologically immediately after nerve crush. A total of six rats were subjected to ON crush, all of which were killed at 14 days.

Tissue processing and histology

All rats were killed by trans-cardial perfusion with physiological saline under deep anaesthesia and, in those rats where tissue was not taken for RT-PCR/Western blotting, subsequently with 4% paraformaldehyde. Initially, the brain was removed. Next, each eye with ON, optic chiasm and the proximal part of the OT attached was carefully dissected. From the dissected tissue, a short piece of ON (2-mm long), 1.5-mm behind the globe, was removed for resin embedding. The brain, globe, remaining ON, chiasm and proximal segment of OT were fixed in 10% buffered formalin for at least 24 h. Following fixation, the brain was positioned in the Kopf rat brain blocker (Kopf Instruments PA001) and 2-mm coronal slices were taken in a dorsal-caudal direction. Brain slices, along with the globe and optic pathway, were processed for routine paraffin-embedded sections. Globes were embedded sagitally; ONs and chiasmata were embedded longitudinally. In all cases, 4-μm serial sections were cut. As detailed above, three rats killed at 2 days were used for transverse sectioning of the ONH. The short piece of proximal ON taken for resin sectioning and toluidine blue staining was treated as previously reported [14].

Immunohistochemistry

Colorimetric immunohistochemistry was performed as previously described [9]. In brief, tissue sections were deparaffinized before treatment with 0.5% H_2O_2 for 30 min to block endogenous peroxidase activity. Antigen retrieval was achieved by microwaving the sections in 10-mM citrate buffer (pH 6.0). Tissue sections were then blocked in PBS containing 3% normal horse serum, incubated overnight in primary antibody, followed by consecutive incubations with biotinylated secondary antibody and streptavidin-peroxidase conjugate. Colour development was achieved with 3′-,3′-diaminobenzidine. Sections were counterstained with haematoxylin, dehydrated and mounted. Specificity of antibody staining was confirmed by incubating adjacent sections with isotype controls (mouse IgG1 and IgG2a isotype controls) for monoclonal antibodies, or normal rabbit/goat serum for polyclonal antibodies.

Double labelling fluorescent immunohistochemistry was performed as previously described [9]. In brief, visualisation of one antigen was achieved using a three-step procedure (primary antibody, biotinylated secondary antibody, streptavidin-conjugated AlexaFluor 594), whilst the second antigen was labelled by a two-step procedure (primary antibody, secondary antibody conjugated to AlexaFluor 488). In summary, sections were prepared as above, except for the omission of the endogenous peroxidase block, then incubated overnight at room temperature in the appropriate combination of primary antibodies. On the following day, sections were incubated with the appropriate biotinylated secondary antibody (1:250) for the three-step procedure plus the correct secondary antibody conjugated to AlexaFluor 488 (1:250, Invitrogen) for the two-step procedure for 30 min, followed by streptavidin-conjugated AlexaFluor 594 (1:500) for 1 h. Sections were then mounted using anti-fade mounting medium and examined under a confocal fluorescence microscope. Primary antibody details are provided in Supplementary Table 1.

Evaluation of histology and immunohistochemistry

All assessments of ON injury were performed in a randomized, blinded manner. Loss of RGC axons in the ONs of glaucomatous eyes was assessed using a semi-quantitative ON grading scheme based on the toluidine blue-stained cross-sections [8, 14], where grade 0 corresponds to no damage, grade 5–50% axon loss, and grade 10–100% axonal loss. Of note, if the calculated damage grade was zero, but the nerve contained at least 20 damaged axons within the whole cross-section, the grade was recorded as 1 as a nominal indication that the nerve was damaged.

β-Amyloid precursor protein (APP) accumulation in the ONH as a result of disrupted axonal transport was assessed semi-quantitatively using a 4-point grading system, ranging from 0 = undetectable to 3 = numerous intensely stained APP-positive axons covering a substantial area of the pre-laminar to post-laminar ONH. The APP score of each rat was then correlated with the peak IOP elevation of that rat and with the IOP at the time of death. Statistical analysis of correlations were performed by GraphPad Prism 5.0b (GraphPad Software Inc., La Jolla, CA) using non-parametric tests.

Quantification of SMI-32 immunolabelling in longitudinal sections of the medial ON and proximal OT was performed as previously described [14]. In brief, immunostained sections, each expressing a representative level of immunoreactivity, were photographed at 200×. They were then imported into NIH Image-J 1.42q software (http://www.rsb.info.nih.gov/ij/), where they underwent colour deconvolution to separate diaminobenzidine reaction product from haematoxylin counterstain [41]. Images were subsequently analysed with regard to the specifically stained area in pixels using the in-built functions of the Image-J software. Statistical analysis was carried out by ANOVA followed by post hoc Tukey's test.

Electrophoresis/Western blotting

The entire ON was taken for Western blotting except for 1.5 mm at the proximal and distal ends; thus, only the

myelinated segment of the nerve was analysed. Retinas and ONs from 3 to 7 days, and ONs from 14-day experimental glaucoma rats were processed for Western blotting as previously described [9]. In brief, after electrophoresis, samples were transferred onto PVDF membranes. Following a block of non-specific binding, blots were probed with primary antibodies (see Supplementary Table 1), appropriate secondary antibodies conjugated to biotin, and streptavidin-peroxidase conjugate. Blots were then developed and the images captured and analysed for densitometry. Densitometry values were normalised for actin. Statistical analysis was performed by Kruskall–Wallis followed by Mann–Whitney for comparison of SMI-32, SMI-37 and SMI-31 expression in 3, 7 and 14 days ON samples and by Student's paired *t* test for Gap43 expression in treated versus control retinas.

Real-time RT-PCR

Reverse-transcription polymerisation chain reaction (RT-PCR) studies were carried out as described previously [11]. In brief, retinas were dissected, total RNA was isolated and first-strand cDNA was synthesised from 2-µg DNase-treated RNA. Real-time PCR reactions were carried out in 96-well optical reaction plates using the cDNA equivalent of 20-ng total RNA for each sample in a total volume of 25 µl containing 1× SYBR Green PCR master mix (Bio-Rad), forward and reverse primers at a final concentration of 400 nM. The thermal cycling conditions were 95°C for 3 min and 40 cycles of amplification comprising 95°C for 12 s, 63°C for 30 s and 72°C for 30 s. Primer sets used were as follows (sense primer, antisense primer, product size, accession number): GAPDH (5′-TGCACCACCAACTGCTTAGC-3′, 5′-GGCATGGACTGTGGTCATGAG-3′, 87 bp, NM_017008), NFL (5′-ATGGCATTGGACATTGAGATT-3′, 5′-CTGAGAGTAGCCGCTGGTTAT-3′, 105 bp, AF031880), Thy1.1 (5′-CAAGCTCCAATAAAACTATCAATGTG-3′, 5′-GGAAGTGTTTTGAACCAGCAG-3′, 83 bp, X03150). After the final cycle of the PCR, primer specificity was checked by the dissociation (melting) curve method. In addition, specific amplification was confirmed by electrophoresis of PCR products on 3% agarose gels. PCR assays were performed using the IQ5 icycler (Bio-Rad) and all samples were run in duplicate. The results obtained from the real-time PCR experiments were quantified using the comparative threshold cycle (C_T) method ($\Delta\Delta C_T$) for relative quantitation of gene expression [27], corrected for amplification efficiency [36]. All values were normalised using the endogenous housekeeping gene GAPDH and expressed relative to controls. Statistical analysis was carried out by ANOVA followed by post hoc Tukey's test. The null hypothesis tested was that C_T differences between target and housekeeping genes would be the same in control and experimental retinas.

Results

Axonal transport disruption at the ONH is an early event during experimental glaucoma

The ONH has long been considered a site of early axonal transport failure in glaucoma [1, 29, 37, 39, 40], but recent data from rodents indicate that distal axons are affected first [12]. To address this important issue, we performed immunolabelling for APP, a protein synthesised by RGCs [30] and conveyed along the ON by fast axonal transport. We found accumulation of APP in axons in the pre- and post-laminar ONH as early as 8 h following induction of raised IOP (Fig. 1a, b). By 24 h, intense APP immunoreactivity was observed throughout the ONH, a result that was typical of the majority of rats analysed within the first 7 d. By 14 d, however, not much APP accumulation was detectable at the ONH in most animals (Fig. 1c–f). To ascertain whether axonal transport disruption correlated with the peak increase in IOP or the terminal IOP, representative sections from the central ONH of every rat were graded for APP accumulation and related to the peak IOP value recorded from that rat and to the IOP at the time of death. A Spearman's rank correlation was then performed. The maximal APP score was documented at 24 h after induction of experimental glaucoma, with similar, somewhat lower values obtained at 3 and 7 days, and a substantially lower grade at 14 days (Table 1). There was no correlation between peak IOP and APP grade ($r = 0.27$, $P = 0.11$). In contrast, the terminal IOP showed a

Table 1 Grading of APP accumulation at the ONH at various times after induction of experimental glaucoma

Time	Cont eyes	8 h ($n = 4$)	1 day ($n = 7$)	3 days ($n = 8$)	7 days ($n = 9$)	14 days ($n = 10$)
Integral exposure IOP[a]	–	–	16.5 ± 2.1	47.1 ± 11.1	97.7 ± 8.7	189.2 ± 13.2
Peak increase in IOP[a]	–	28.5 ± 2.7	24.2 ± 4.6	25.8 ± 5.4	26.3 ± 2.5	24.2 ± 2.2
IOP increase at time of death[a]	–	28.0 ± 3.0	21.5 ± 4.0	15.0 ± 7.0	13.3 ± 2.6	5.0 ± 1.3
APP grade	0.0 ± 0.0	1.5 ± 0.3	3.8 ± 0.2	2.9 ± 0.3	2.7 ± 0.2	1.5 ± 0.2

[a] Calculated as IOP of treated eye—IOP of untreated contralateral eye and expressed in mmHg

significant correlation with the APP grade ($r = 0.47$, $P = 0.004$). The results indicate, as expected, that elevated IOP at the time of death is a risk factor for axonal transport disruption. It is, however, noteworthy that the correlation between APP grade and terminal IOP ($r = 0.47$) was not high, indicating that considerable variation exists between rats with regard to how raised IOP affects axonal viability.

We next sought to identify the spatial distribution of axonal transport failure. To ascertain whether axonal transport disruption is restricted to the ONH, we performed double labelling immunohistochemistry of APP with myelin basic protein (MBP) in both longitudinal (Fig. 2a–c) and transverse sections of the ONH and proximal ON (Fig. 2d–i). The results clearly showed that APP immunoreactivity was not associated with the myelinated portion of the ON. In addition, it was apparent that APP accumulation in the lamina was not uniform, but regionalised and asymmetric (Fig. 2h), a result that corresponds with previous findings of regionalised RGC and axonal loss in the DBA/2J mouse [16, 44]. To identify whether any distal parts of the optic pathway feature axonal transport disruption, medial and distal sections of the ON and OT were immunostained for APP. Images of the ONH, medial ON and proximal OT from a typical 3-day rat are shown (Fig. 2j–l). No sites of APP accumulation were detected beyond the ONH at any time point, indicating the crucial significance of this structure in the pathology of experimental glaucoma.

To further characterise the nature of axonal transport disruption during experimental glaucoma, we performed immunostaining for two additional molecules, synaptophysin and brain-derived neurotrophic factor (BDNF), that are synthesised by RGCs and undergo anterograde, fast axonal transport [6, 31]. Synaptophysin displayed broadly similar patterns of accumulation at the ONH as APP, although differences were evident. APP was observed in highest amounts in the pre-laminar ONH and in axons at the margins of the ONH; synaptophysin extended further into the ONH and was distributed more evenly (Fig. 3b–i). BDNF also accumulated at the ONH, but was in lower abundance than APP and was largely pre-laminar. BDNF and synaptophysin both colocalized with APP (Fig. 3d–f, j). The results suggest that all molecules undergoing anterograde fast axonal transport are disrupted by chronic IOP elevation. To confirm that accumulations of APP and synaptophysin represent disrupted fast axonal transport, we performed double labelling in ocular hypertensive rats that had been labelled with the neural tracer cholera toxin β-subunit (CTB). After 2 days of experimental glaucoma, CTB was associated with RGC somata, dendrites and axons, and accumulated at the ONH in many of the same axons as APP and synaptophysin (Fig. 3g–i). Double labelling of APP with microglial and astocytic markers (Fig. 3k, l) failed to show any colocalisation indicating APP immunoreactivity resided solely within axons.

Characterisation of axonal cytoskeleton damage during experimental glaucoma

Our next goal was to define the temporal relationship between disrupted axonal transport and damage to the ON

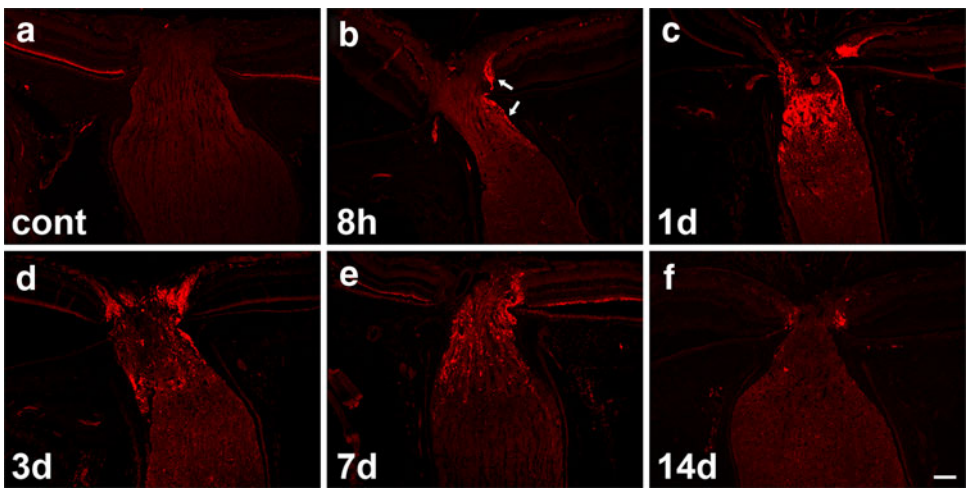

Fig. 1 Accumulation of APP at the ONH at various times following induction of experimental glaucoma. In normal rats, APP immunoreactivity is localised to RGC bodies, but only very low intensity labelling is associated with RGC axons in the ONH and ON (**a**). By 8 h after induction of chronic ocular hypertension, accumulation of APP is evident within some axons in the pre- and post-laminar ONH (**b** *arrows*). At 24 h, intense APP immunoreactivity is typically observed throughout the ONH (**c**). Analysis of rats at 3 d (**d**) and 7 d (**e**) shows APP immunolabelling in the ONH remains high, although not as widespread as 1 day. By 14 days after induction of experimental glaucoma (**f**), not much APP immunoreactivity is observed in the pre- or post-laminar ONH. *Scale bar* 100 μm

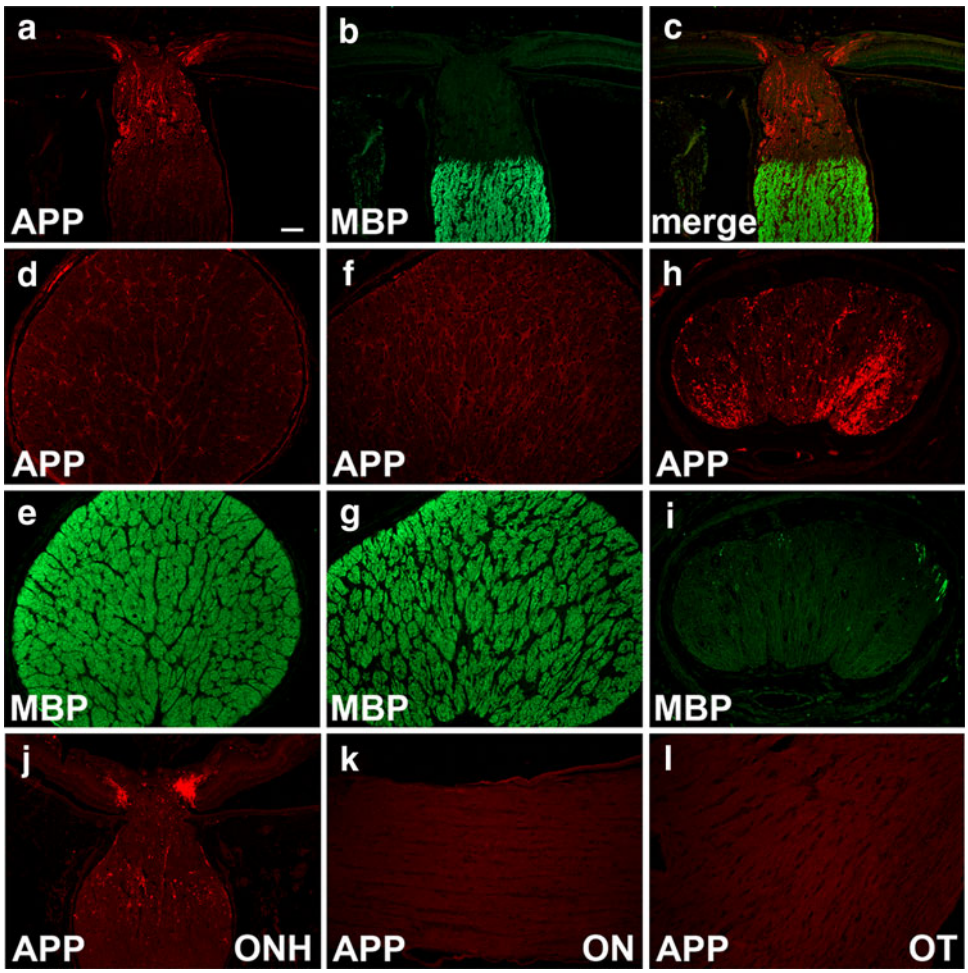

Fig. 2 APP accumulation is restricted to the ONH during experimental glaucoma. **a**–**i** Feature double labelling immunohistochemistry of APP (*red*) with MBP (*green*) showing that axonal transport disruption occurs only within the initial, non-myelinated portion of the nerve; **a**–**c** highlight the ONH and proximal ON of a rat killed 7 days after induction of experimental glaucoma in longitudinal orientation; **d**–**i** show three levels of the proximal ON of a typical 2 day rat in cross-sectional plane, where transverse sections were taken through the ON at 400 μm intervals in a distal to proximal direction showing the mature myelinated ON (**d**, **e**), the early portion of the myelinated ON (**f**, **g**) and the unmyelinated lower neck region (**h**, **i**), which features widespread APP immunolabelling. A rat killed after 3 days of ocular hypertension: APP accretion is clearly visible at the ONH (**j**), but not more distally in the ON (**k**) or OT (**l**). *Scale bar* **a** and **d**–**f** 100 μm, **b**, **c** and **g**–**l** 50 μm

axonal cytoskeleton. This provides information on whether axonal transport deficiencies are functional or mechanical. The standard methodology for evaluating ON injury is quantitative evaluation of transverse sections of the proximal nerve stained with toluidine blue [33]. Accordingly, we analysed ONs for damage at increasing times after induction of raised IOP (Fig. 4). At 1 day, when axonal transport disruption is maximal, there was no evidence of any axonal abnormalities. Between 3 and 14 days, axonal disruption increased dramatically, which was manifest initially as the enlargement of a few axons, then progressed to the appearance of hyperdense axons, myelin disruption and reduced axon density.

The toluidine blue methodology is well suited to identifying gross abnormalities and axonal loss; however, it may lack the sensitivity to detect early or subtle axonal injury. An alternative, complementary technique involves analysis of longitudinal sections immunostained for specific markers of the axonal cytoskeleton. This approach is routinely employed for delineation of axonal damage in other white matter tracts. Initially, we evaluated the sensitivity and efficacy of eight immunohistochemical markers for detection of early ON damage. SMI-32, an antibody that recognises the heavy chain of non-phosphorylated neurofilament (npNFH), was unequivocally the most sensitive indicator. This was the case both at 3 and 7 days, in rats with slight damage and in rats with numerous abnormalities. The pattern of SMI-32 immunolabelling changed from one consisting of light, uniform staining of axons to one featuring axonal beading, swellings and spheroids. Representative images of the eight markers in sections from the medial ON of a 3-day rat with only a small number of injured fibres are shown (Supplementary Fig. 1a).

Next, we utilised SMI-32 to quantify axonal damage. Sections from the medial ON and proximal OT of 1, 3 and 7 days rats were immunolabelled for SMI-32 (see Supplementary Fig. 1b for typical staining patterns), and the extent of abnormalities calculated. The results, revealed no evidence of axonal injury in either location at 1 day, but significant damage by 3 days, and fourfold greater damage by 7 days (Table 2). Comparison of the ON with the OT showed the mean damage level in the OT was somewhat higher than the ON at the 3-day time point, but there was

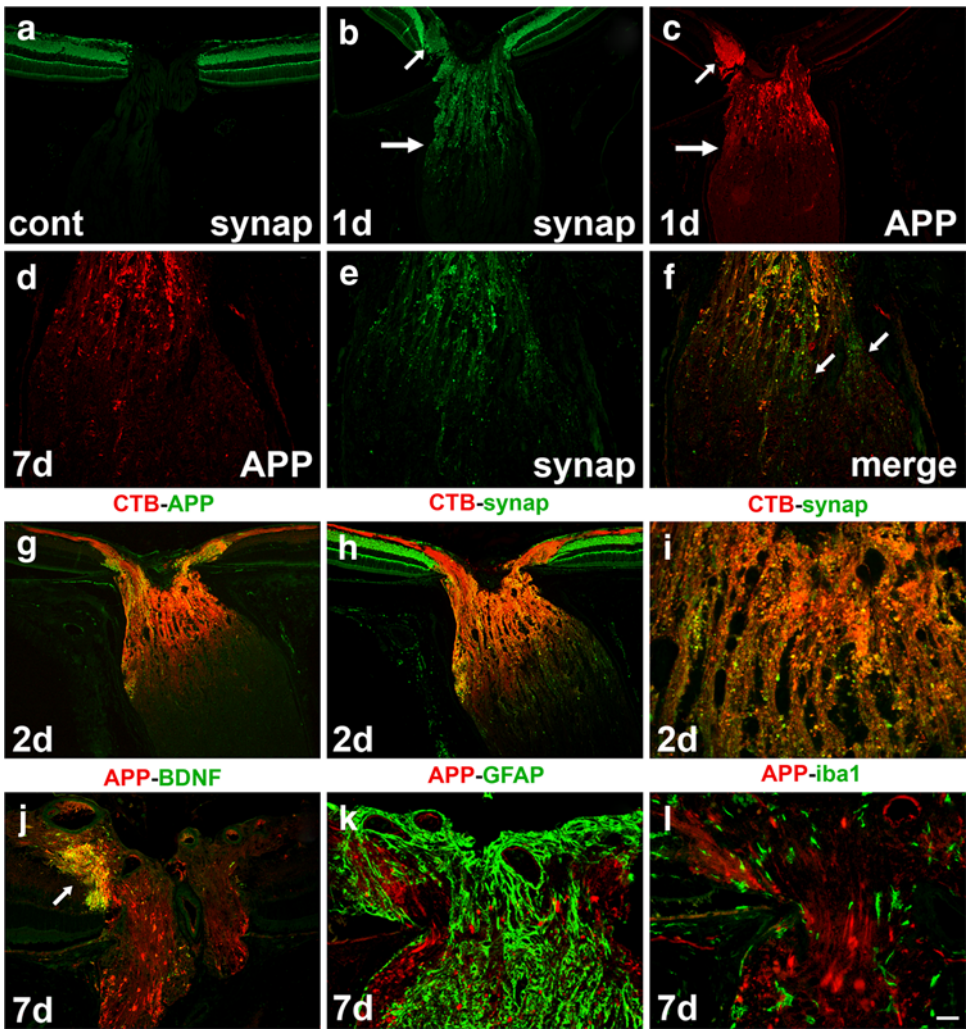

Fig. 3 Comparison of APP with other markers of axonal transport disruption after induction of experimental glaucoma. In normal rats, synaptophysin immunoreactivity is localised to post-synaptic terminals in the retina, but only very low intensity labelling is associated with RGC axons in the ONH and ON (**a**). At 24 h after induction of experimental glaucoma, accumulation of synaptophysin (**b**) is observed throughout the ONH in a similar pattern to APP (**c**). Synaptophysin colocalises with APP, as seen in this rat killed at 7 days (**d–f**). At 2 days after induction of experimental glaucoma, CTB (**g–i** *red*) is associated with RGC somata, dendrites and axons in the retina and accumulates throughout the ONH. CTB colocalises with APP (**g** *green*) and with synaptophysin (**h**, **i** *green*). In every rat, synaptophysin immunoreactivity extends further into the ONH than APP (**b**, **c**, **f**, **h** *arrows*). BDNF (**j** *green*) also colocalises with APP (**j** *red*), predominantly in the pre-laminar ONH (*arrow*). In contrast, the astrocytic marker GFAP (**k** *green*) and the microglial marker iba1 (**l** *green*) do not colocalise with APP (**k**, **l** *red*). *CTB* cholera toxin β-subunit. *Scale bar* **a–c**, **j**, **k** 100 μm, **d–f** 50 μm, **g–i** l, 25 μm

no difference at 7 days. A number of conclusions can be drawn: first, SMI-32 and toluidine blue provided complementary results; secondly, despite axonal transport disruption at the ONH commencing by 8 h, no axonal cytoskeletal abnormalities were evident in the myelinated nerve at 24 h; thirdly, degeneration may have commenced, or proceeded more rapidly, in the distal part of the axon.

The SMI-32 analyses described above relate to the central portion of the visual pathway. To better understand whether the primary locus of axonal degeneration is at the distal or the proximal end of pathway, it is necessary to analyse the entire tract, from the ONH to the lateral geniculate nucleus and superior colliculus. Accordingly, we performed a spatial assessment of SMI-32 immunostaining in rats subjected to experimental glaucoma. The results were as follows: (1) no alterations to SMI-32 immunostaining were noted in the visual pathway at 8 h; (2) at 1 d, SMI-32 abnormalities, visualised as beading and swellings, were evident in the pre-laminar and laminar ONH in some, but not all animals, however, no such abnormalities were manifest distal to this location in the entire myelinated ON and OT; (3) after 3 days, SMI-32 abnormalities were apparent throughout the length of the white matter tract from the ONH via the optic chiasm to the brachium of the superior colliculus. Figure 5 shows representative images from the ONH, optic chiasm and distal

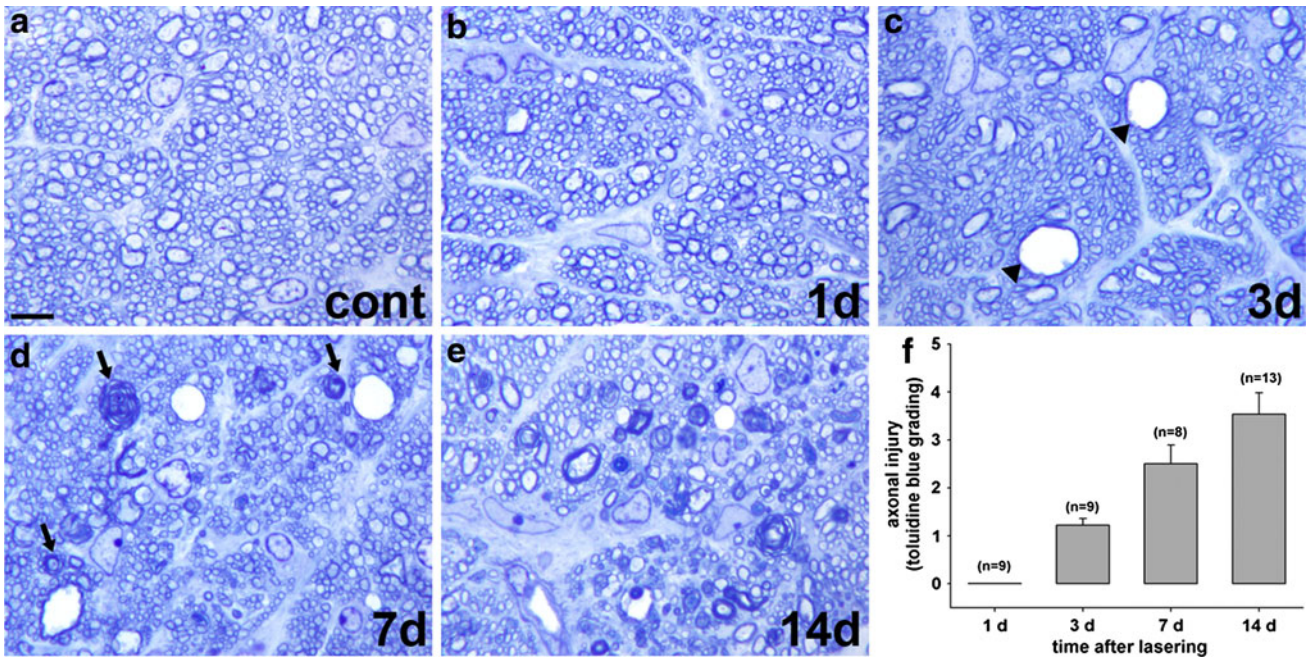

Fig. 4 Transverse sections of ONs stained with toluidine blue at various times subsequent to induction of experimental glaucoma. At 1 day after induction of chronic ocular hypertension (**b**), the axonal structure is unchanged relative to control ONs (**a**). By 3 days, a few enlarged axons (*black arrowheads*) are typically visible (**c**). After 7 days of experimental glaucoma, reduced axon density and myelin disruption (*black arrows*) are evident (**d**), features that are even more prevalent after 14 days of raised pressure (**e**). Mean axonal injury at increasing times after induction of experimental glaucoma is shown (**f**). *Scale bar* 25 μm

Table 2 Quantification of SMI-32 abnormalities at various times after induction of experimental glaucoma

Time	Control	1 day	3 days	7 days
Medial ON	0.39 ± 0.28	0.13 ± 0.13	24.7 ± 7.2	106.7 ± 31.0†
Proximal OT	0.40 ± 0.17	0.38 ± 0.30	37.0 ± 9.1*	110.5 ± 26.7†

Immunoreactivities were quantified (see "Materials and methods") and expressed as area in pixels ($\times 10^3$)

All values are presented as mean ± SEM, where $n = 9$ (control), $n = 8$ (1 day), $n = 10$ (3 days), $n = 9$ (7 days)

Statistical analysis of immunoreactivities was performed by ANOVA followed by a post-hoc Tukey's test for multiple comparisons

Significant differences versus controls are indicated by * $P < 0.05$ and † $P < 0.001$

OT. To confirm axonal cytoskeletal abnormalities at the ONH at 1 day, sections were also immunostained for neurofilament medium. The pattern of abnormalities produced was almost identical to SMI-32 (data not shown). The overall results indicate that axonal cytoskeleton changes occur first at the ONH.

There is debate as to whether increased or decreased neurofilament phosphorylation signifies injury in neurodegenerative diseases in general [35] and glaucoma in particular [22, 42, 45]. As described above, we observed numerous npNFH (SMI-32) abnormalities in ON sections; however, it is unclear whether this represents an overall dephosphorylation of NFH or merely breakdown of the more labile non-phosphorylated subunit. Thus, we undertook Western blotting in ON samples from control and treated eyes using two antibodies, SMI-32 and SMI-37, which exclusively recognise npNFH (Fig. 6). Each antibody detected a protein of 200 kDa signifying native npNFH, but in treated ONs, a continuum of lower molecular weight proteins reactive to SMI-32 and SMI-37 was also observed. Densitometry showed no significant (SMI-32, $P = 0.42$; SMI-37, $P = 0.24$) difference in the intensity of the 200 kDa species between the 3, 7 and 14-day time points. In contrast, there was a marked increase in intensity of the lower molecular weight products over the time period analysed (SMI-32, $P = 0.036$; SMI-37, $P = 0.011$). The data indicate that there is no increase in npNFH in the ON during ocular hypertension-induced axonal degeneration, rather there is a progressive degradation of npNFH. Western blots performed using the antibody SMI-31, which exclusively recognises pNFH, failed to reveal a continuum of lower molecular weight protein bands.

The ONH is the site of putative axonal regeneration failure during experimental glaucoma

In the ON, axonal injury is not followed by any beneficial regeneration. Severed or crushed RGC axons display only

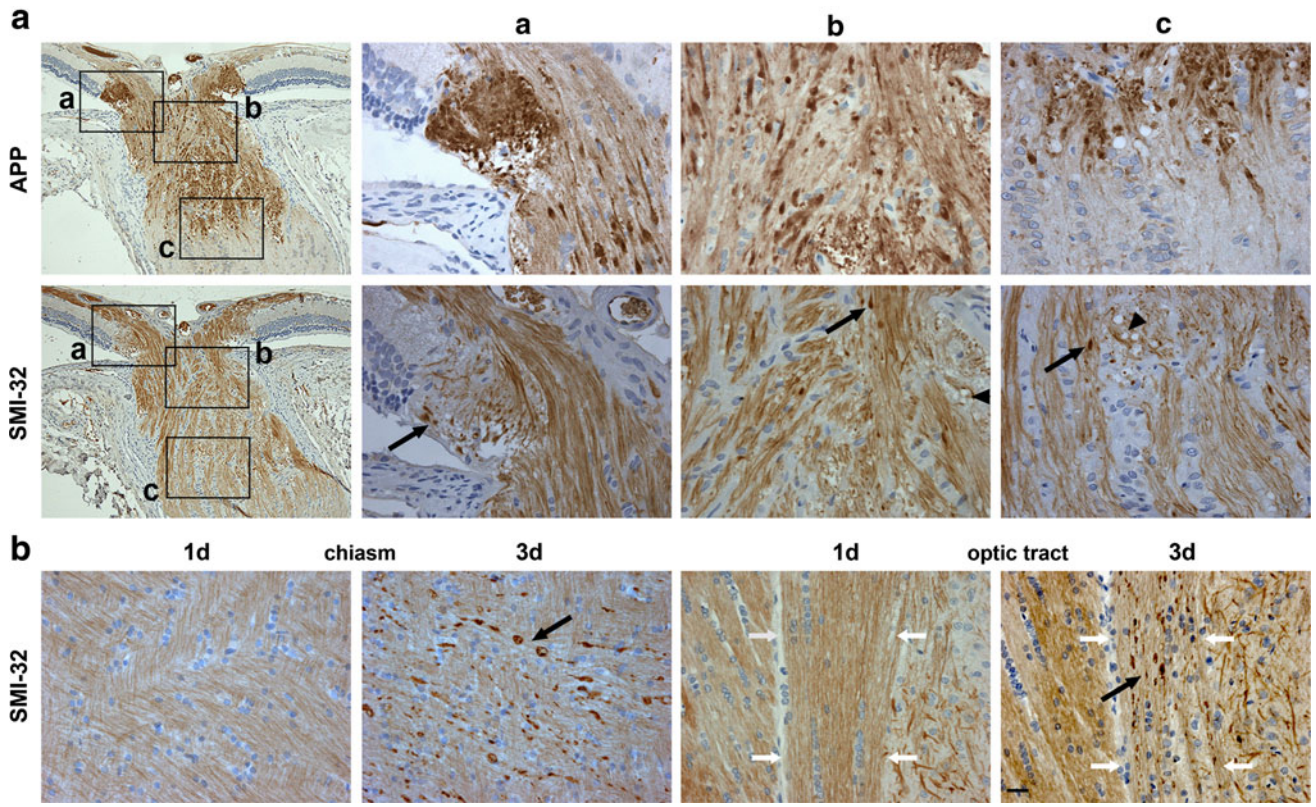

Fig. 5 Axonal degenerative changes in the visual pathway at early time points during experimental glaucoma. **a** Representative images of APP and SMI-32 staining in three regions of the ONH at 1 day after induction of chronic ocular hypertension. At 1 day, widespread APP accumulation is evident in axons throughout the ONH. SMI-32-labelled axon fibres show swellings and beading (*arrows*) and vacuolization (*arrowhead*) in areas of axonal transport disruption. **b** Representative images of SMI-32 staining at the level of the optic chiasm and optic tract 1 and 3 days after induction of chronic ocular hypertension. Unlike the ONH, the myelinated ON and optic tract appear normal at 1 day. By 3 days, SMI-32 abnormalities are evident throughout the length of the white matter tract (*black arrows*). The boundaries of the optic tract are demarcated by *white arrows*. *Scale bar* **a** ONH overview, 45 μm, magnified images, 16.7 μm, **b** 25 μm

transient, local sprouting proximal to the site of damage [3]. Unlike ON crush or transection, RGCs are lost gradually during experimental glaucoma; moreover, the locus of injury to RGCs is unclear. Thus, evaluation of the spatiotemporal pattern of any endogenous axonal regeneration that occurs during glaucoma will be greatly informative to our understanding of the pathology of the disease. To achieve this objective, we analysed expression of growth-associated protein 43 (Gap43), the classical marker of axonal regeneration in the ON [4, 13, 25].

In normal adult rats, negligible Gap43 immunoreactivity was associated with RGC bodies or their axons (Fig. 7a). The situation was unchanged at 24 h after induction of raised IOP, even in rats with widespread axonal transport disruption and neurofilament damage (Fig. 7b). By 3 days, limited Gap43 immunohistochemistry was detectable in RGC axons of some rats, particularly at the level of the prelaminar ONH (Fig. 7c), whilst Western blotting showed that all rats analysed had a markedly upregulated level of retinal Gap43 protein (Fig. 8a, b). The expression of Gap43 increased further at 7 and 14 days, as evidenced by immunohistochemistry (Fig. 7d–i) and Western blotting (Fig. 8a, b). The pattern of Gap43 immunoreactivity in ocular hypertensive rats was broadly equivalent to that of APP with accumulation throughout the ONH, but was significantly delayed in onset. Although APP immunostaining was maximal at 1 day and then gradually declined, the opposite occurred for Gap43. Unlike APP, a few Gap43-positive axons extended beyond the ONH into the initial myelinated portion of the ON (Fig. 6f). Nevertheless, Western blotting (Fig. 8b) showed no measureable increase in the Gap43 content of the myelinated ON at 7 days. The overall results suggest that injured RGCs attempt to regenerate their axons during experimental glaucoma, but the process fails at the ONH. A caveat to this conclusion is that Gap43 expression alone is not conclusive of axonal regeneration. To verify that injured RGCs, rather than healthy cells, are responsible for re-instigating Gap43 expression, we performed double labelling of Gap43 with heat shock protein 27 (Hsp27) in retinas subjected to 14 days of experimental glaucoma. Hsp27, a molecular chaperone induced by cellular stress, is not constitutively

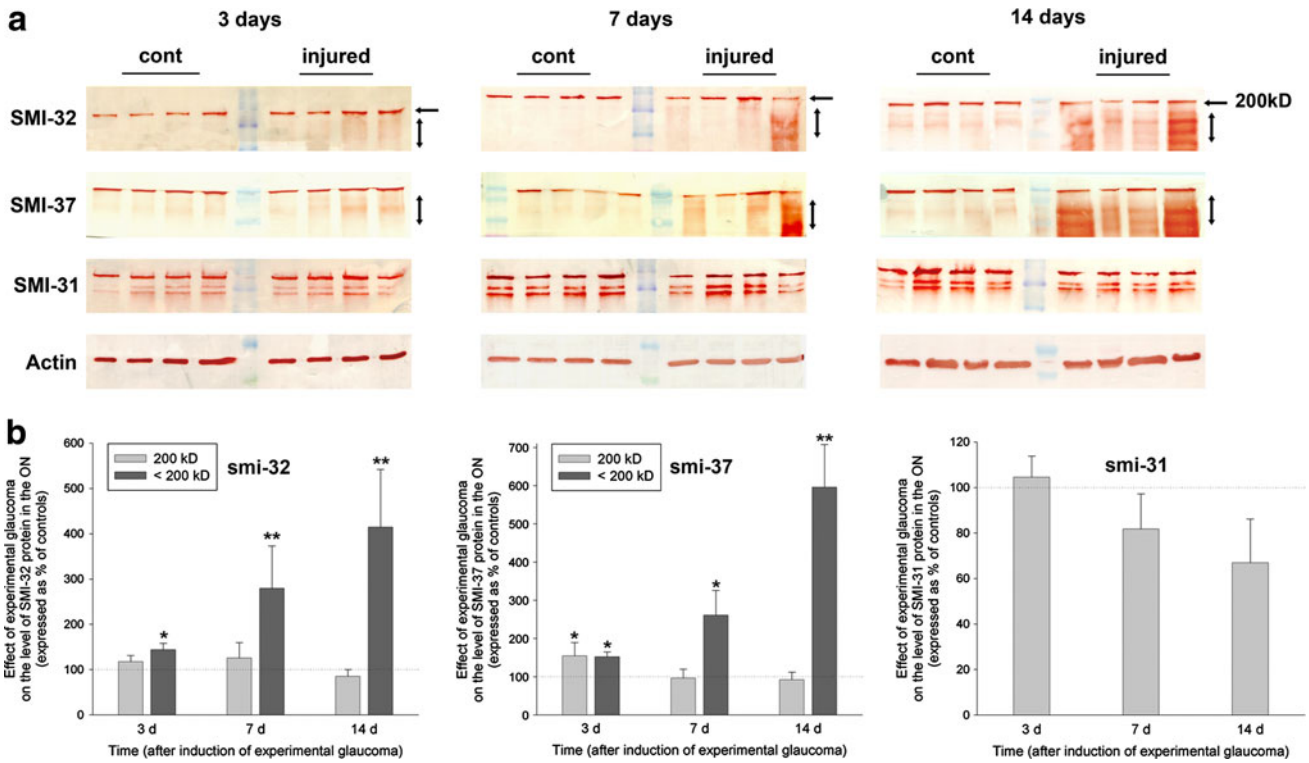

Fig. 6 Expression of npNFH and pNFH in the ON following induction of experimental glaucoma, as evaluated by Western blotting using two antibodies, SMI-32 and SMI-37, that recognise npNFH and one antibody, SMI-31, that recognises pNFH. **a** Representative blots from control and treated ONs from four animals killed at 3, 7 and 14 days are shown. Both antibodies recognise a 200 kDa band that represents native npNFH. A continuum of lower molecular weight bands reactive to SMI-32 and SMI-37, but not SMI-31, are visible in the treated ONs, as indicated by the *vertical arrows*. **b** Densitometry measurements (normalised for actin and expressed relative to the control ON) are provided in the *graphs* below, where $n = 7$ (3 days), $n = 7$ (7 days) and $n = 4$ (14 days). $^{*}P < 0.05$, $^{**}P < 0.01$ compared with controls by Mann–Whitney U test

expressed by RGCs; however, within an ongoing pathological setting, such as axotomy or glaucoma, is persistently upregulated in severely injured RGCs [21, 24]. The results showed that many RGCs were immunopositive for both Hsp27 and Gap43 (Fig. 8c) indicating their increased stress status.

The pattern of injury during experimental glaucoma displays pathological similarities to optic nerve crush, but not to NMDA-induced excitotoxicity.

Hitherto, it is unclear whether degeneration of RGC axons precedes degeneration of RGC somata during glaucoma. Whilst a body of evidence supports this hypothesis, other data endorse the view that atrophy of RGC perikarya occurs first [45]. To elucidate the timing of RGC somatic injury, we performed a temporal analysis of RGC gene expression during experimental glaucoma. The rationale for this approach is that down-regulations of RGC-specific mRNAs, including Thy1 and neurofilament light (NFL), are sensitive early indicators of RGC viability [10, 43]. Following induction of raised IOP, negligible down-regulation of Thy1 and NFL had occurred by 24 h (Fig. 9a). By 3 days, the levels of both mRNAs had decreased, but the changes failed to reach statistical significance. After 7 days, highly significant ($P < 0.001$) decreases of Thy1 and NFL were measured. The time courses of these changes are delayed compared with the axonal responses described above, indicating that altered gene transcription occurs subsequent to axonal disruption.

To impart perspective on the results, we assessed RGC gene expression, disruption of axonal transport and damage to the axonal cytoskeleton in rats that underwent NMDA-induced excitotoxicity. NMDA treatment is the classical method of eliciting somato-dendritic death of RGCs, since NMDA receptors are present on the soma but not the axon of the RGC. Moreover, excitotoxicity is implicated in the pathogenesis of glaucoma [7]. The results were in complete contrast to those of the glaucoma model. Down-regulation of Thy1 and NFL mRNAs was in evidence as early as 6 h after NMDA administration and by 24 h both mRNAs were maximally down-regulated, signalling death of the RGC soma (Fig. 9b). Despite the fatal injury to the RGC body, no disruption to the axonal cytoskeleton, either at the ONH or within the ON, was detectable at 24 h after NMDA administration (Fig. 9c). By 2 days, however, axonal

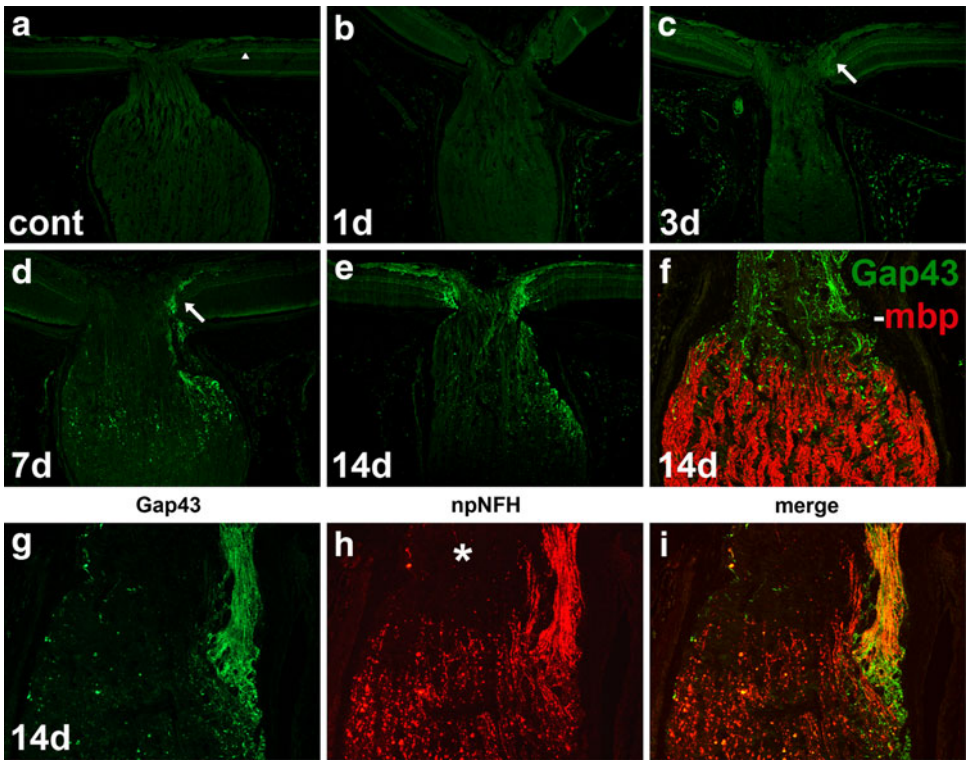

Fig. 7 Gap43 expression in RGC axons following induction of experimental glaucoma. In control rats (**a**), minimal Gap43 immunoreactivity is associated with RGC bodies or their axons, but a lamina of punctae is visible in the inner plexiform layer at the border with the INL (*arrowhead*). No discernible alteration to the pattern of Gap43 staining is evident at 1 day (**b**) after induction of chronic ocular hypertension. By 3 days (**c**), occasional Gap43-immunopositive fibres are apparent in the pre-laminar ONH of some rats (*arrow*). After 7 days (**d**), numerous axons in the pre- (arrow) and post-laminar ONH label for Gap43. Three representative rats are shown after 14 days of experimental glaucoma: the first rat (**e**) displays intense Gap43 immunoreactivity in the nerve fibre layer and within the ONH; the second rat (**f**) displays abundant Gap43-positive axons throughout the ONH with a few axons extending into the initial myelinated portion of the ON (Gap43, *green*, *mbp red*). The third rat (**g**–**i**) has substantial axonal loss in the ONH (*highlighted by asterisk*) and features robust Gap43 labelling of surviving axons in this region of the ON. *Scale bar* **a**–**e** 100 μm, **f**–**i** 50 μm

swelling and beading was visible throughout the entire ON and OT (Fig. 9d). Unlike experimental glaucoma, no accumulation of APP occurred at the ONH following NMDA treatment (Fig. 9e). The overall results show the two paradigms of RGC death have quite distinct pathologies.

Further evidence illustrating the different injury profiles of experimental glaucoma and excitotoxicity was provided by comparison of their Hsp27 and Gap43 responses (Supplementary Fig. 2a, b), which, as discussed above, can be viewed as indicative of ongoing somatic and axonal injury, respectively. After 14 days of chronic ocular hypertension, a proportion of surviving (β_3-tubulin-labelled) RGCs expressed Hsp27 and synthesized Gap43. In contrast, 7 days after NMDA administration, surviving RGCs were Hsp27- and Gap43-negative. Thus, excitotoxicity causes acute, fatal injury to a proportion of RGCs, but surviving RGCs are somatically and axonally healthy, whilst glaucoma damages the axon, but spares the soma of a proportion of RGCs, leading to ongoing perikaryal stress and delayed death. To ascertain whether the response seen during glaucoma is characteristic of ON crush, we also analysed rats subjected to intraorbital ON crush 14 days previously. Similar to glaucoma, RGCs from ON crush rats expressed Hsp27 and synthesized Gap43 (Supplementary Fig. 2a, b). When compared with glaucoma, substantially more Gap43 immunoreactivity was observed, which extended well beyond the ONH. This is to be expected; however, as the entire population of RGCs is affected by crush and the site of crush was 3 mm distal to the ONH.

Discussion

In the current study, we have employed a rat model of optic neuropathy induced by chronic elevation of the IOP together with a combination of histology, immunohistochemistry, Western blotting and real-time RT-PCR to address the spatial and temporal nature of RGC pathology. As identified by Morrison et al. [33], the advantage of such a model compared with spontaneous models of chronic ocular hypertension is that the timing of the IOP increase following

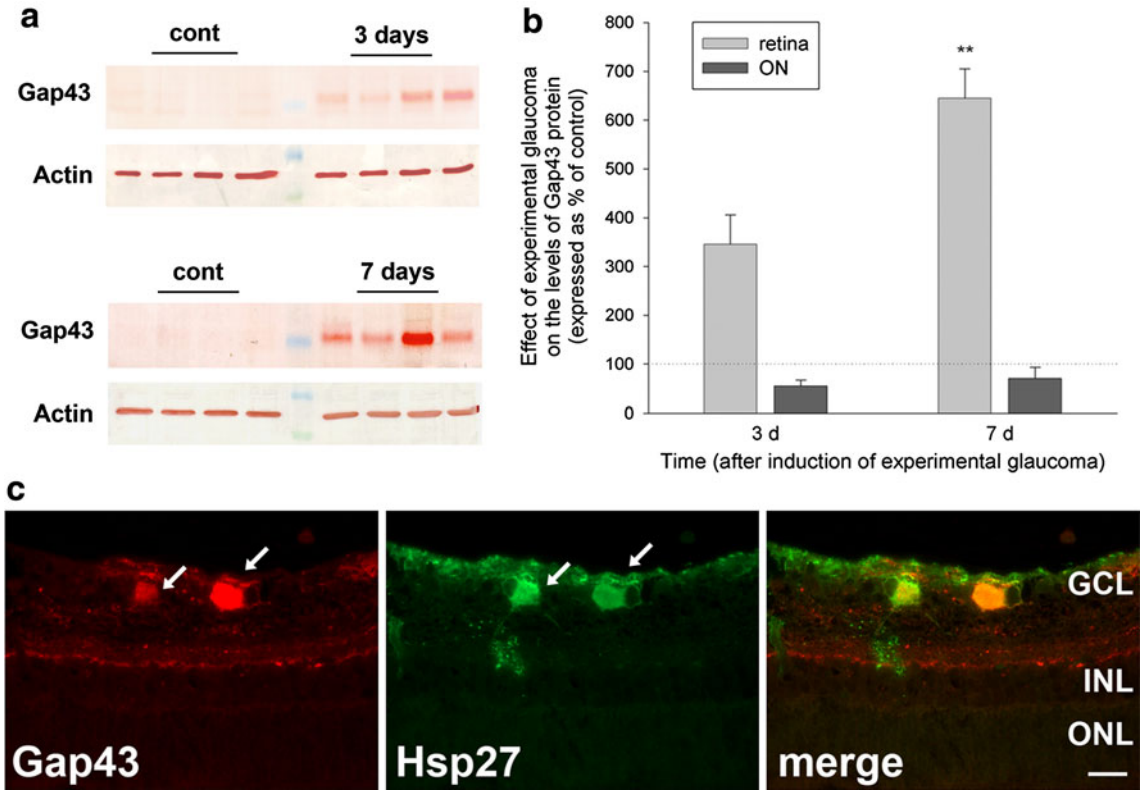

Fig. 8 Gap43 expression in the retina and ON following induction of experimental glaucoma. **a** Expression of Gap43 in the retina as evaluated by Western blotting. Representative blots from control and treated retinas from four animals killed at 3 and 7 days after induction of chronic ocular hypertension are shown. **b** Densitometry measurements (normalised for actin and expressed relative to the control eye) for retinas and ONs are shown in the accompanying *graph*, where $n = 7$. $^{**}P<0.01$ by paired Student's t test (control vs. treated). **c** Double labelling immunofluorescence of Gap43 with Hsp27 in a representative rat killed 14 days after induction of experimental glaucoma. Gap43-positive RGCs frequently express Hsp27. *GCL* ganglion cell layer, *INL* inner nuclear layer, *ONL* outer nuclear layer. *Scale bar* 25 μm

the surgical intervention is known. This engenders greater confidence in conclusions drawn about the chronology of pathological events. The data presented here provide robust support for the hypothesis that the ONH is the pivotal, and likely the primary, site of RGC injury following moderate elevation of IOP, with resulting anterograde degeneration of axons and retrograde injury and death of somas.

Anterograde fast axonal transport conveys newly synthesized molecules away from the cell body. Obstruction of this process rapidly compromises the integrity of the distal axon. In glaucoma, the lamina cribrosa of the ONH has long been considered a likely site of axonal transport failure. This hypothesis was formed after pioneering work performed in monkeys, which demonstrated that radioactive leucine accumulated within axons at the ONH after moderate elevation of IOP [1, 29, 37, 38, 40]. Similar results have been found in pigs [2]. However, current glaucoma research is mainly performed in rodents, and rodents lack a true lamina cribrosa. Rats possess a rudimentary structure, whilst mice have no connective tissue [15, 32]. As such, it is important to ascertain whether the ONH is an important site of axonal transport failure in rodents. We achieved this aim by immunolabelling for proteins (APP, synpatophysin and BDNF) that are routinely synthesised by RGCs and conveyed along the ON by fast axonal transport [6, 31]. Because the molecules analysed are of different molecular weights and have distinct physiological roles, this approach provides biologically meaningful information about transport viability during chronic ocular hypertension. Our results showed accumulation of all three proteins within axons at the ONH, but not distal to this location in the myelinated ON or OT, results confirmed by the use of the neural tracer CTB. The time course correlated well with the early monkey studies, with detectable accumulation by 8 h and widespread dysfunction from 24 h. By 14 days, however, the mean IOP had decreased markedly and disruption was measurably lower. The reduced accumulation of APP at this time point can be accounted for in two ways: (1) in axons that were not irreversibly damaged, the lower IOP allows normal transport of APP to resume; (2) axons that were irreversibly damaged by high IOP have now degenerated. Quigley and

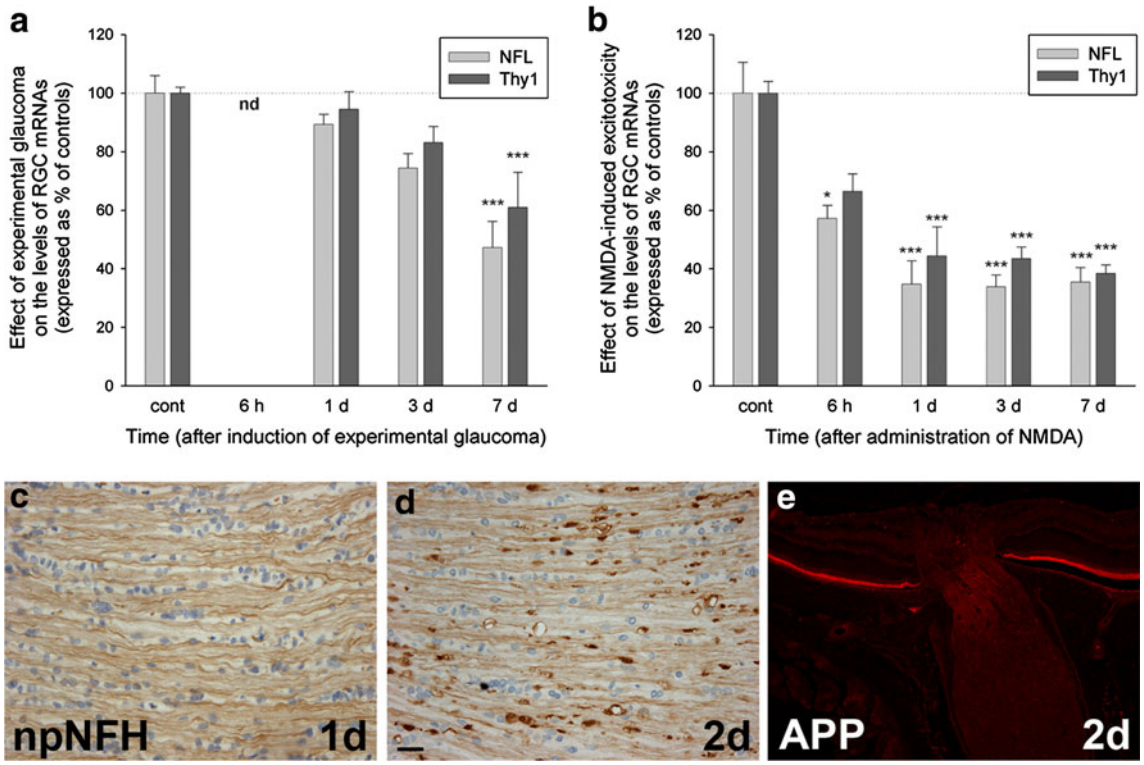

Fig. 9 Temporal characterisation of downregulation of the RGC-specific mRNAs Thy1 and NFL in the retina following induction of experimental glaucoma (**a**, $n = 4$–9) and NMDA-induced excitotoxicity (**b**, $n = 6$–7), as determined by quantitative real-time RT–PCR. $^{*}P < 0.05$, $^{***}P < 0.001$ by one-way ANOVA followed by post hoc Tukey's test. **c**–**e** Evaluation of axonal degeneration and axonal transport disruption in the ONH after NMDA-induced excitotoxicity. At 1 day after NMDA treatment, SMI-32 (npNFH) immunostaining throughout the ONH and ON appears normal (**c**). By 2 days, numerous axonal swellings and abnormalities are visible throughout the white matter tract (**d**). No accumulation of APP is evident at the ONH following administration of NMDA, as shown in this rat killed at 2 days (**e**). *Scale bar* **c**, **d** 25 μm, **e** 100 μm

Addicks [38] noted that a return to normal IOP within 1 week restored transport in some axons in monkeys.

Previous studies in rats have found results compatible with the hypothesis that chronically elevated IOP disrupts active retrograde axonal transport to the retina at the level of the ONH [28, 42], findings consistent with this study. In contrast, Crish et al. [12] showed that axonal transport dysfunction in both spontaneous and induced rodent models of IOP elevation appeared first at the superior colliculus and progressed distal proximal, with ONH deficits occurring much later. The disparity between these studies may relate to the models used. In the micro-bead model used by Crish et al., the IOP elevations were maximally 10 mmHg and maintained for long periods, whilst the laser model used here and by others produces typical IOP rises of 25 mmHg for shorter periods. It is possible that modest, prolonged increases in IOP gradually compromise axonal transport efficiency, which is first manifest at the distal synapses, whilst greater increases in IOP physically constrict axons at the ONH.

We found axonal cytoskeletal abnormalities, including neurofilament beading and swellings, in the ONH at 24 h after induction of raised IOP. This suggests that axonal transport disruption is mechanical, and not simply functional, in a subset of axons at very early time points. Nevertheless, in other axons, it is likely that active axonal transport dysfunction significantly preceded physical damage, an argument supported by the results of Salinas-Navarro et al. [42], who counted fewer RGCs in retinas back-labelled by a tracer that undergoes active transport than in retinas back-labelled by a passively diffusing tracer. In contrast to the ONH, no axonal cytoskeletal abnormalities were present in the entire myelinated ON and OT until 3 days, with progressively greater damage at 7 and 14 days. The results support the findings of others that IOP elevations of the magnitude recorded in this study elicit an early insult at the lamina of the ONH with Wallerian-like degeneration of axons distal to the site of injury [16, 20, 38]. Regarding axonal cytoskeletal degeneration, a previous study in monkeys showed accumulation of npNFH in the ON following raised IOP [22]. Using immunohistochemistry, we found a similar, robust increase in npNFH labelling in degenerating axons; however, Western blotting of ON samples revealed no increase in the npNFH 200-kDa

band, rather the appearance of a continuum of low-molecular weight bands. These bands almost certainly represent breakdown products and may account for the increased immunoreactivity in tissue sections. npNFH is more labile and sixfold more susceptible than pNFH to degradation by calpain [34] and our data indicate that it degenerates more rapidly than pNFH.

The strikingly early nature of pathological changes at the ONH prompted the question as to whether RGC somas are irreversibly injured at this same time. Our data indicate not. Down-regulation of RGC-specific mRNAs, which are sensitive early indicators of RGC viability [10, 16, 43], occurred subsequent to axonal changes at the ONH and markedly later than in retinas subjected to NMDA-induced somatic excitotoxicity. It can be argued that the elevated IOP placed a considerable physiological stress on a proportion of RGC somas as evidenced by their upregulation of the molecular chaperone Hsp27; yet, this response also occurred in rats with normal IOPs that underwent ON crush and may simply have been caused by damage to the axonal compartment.

The long-term objective of glaucomatous pharmacotherapy is not merely neuroprotection of surviving RGCs, but regeneration of injured/disconnected axons. Within the CNS, endogenous regenerative attempts are always unsuccessful. In the visual system, RGC axons display only transient, local sprouting, proximal to the lesion site after ON crush [3], and interestingly, even this limited response occurs only when the injury is within 3 mm of the eye, not if it is administered to the distal ON [13]. Unlike the catastrophic injury caused by traumatic axonopathies, such as ON crush, RGCs are lost gradually during chronic ocular hypertension and only a proportion of the population will die. It follows that the inhibitory environment for regeneration may be less pronounced and regeneration strategies more effective. Surprisingly, no data are available on the endogenous regenerative response of RGCs during experimental glaucoma. Delineating such information is of utmost importance. We have shown in the current study that RGC axonal injury is first evident at the ONH and that the somas remain viable for a number of days; thus, we hypothesised that endogenous RGC regeneration should proceed at least to the ONH. To examine putative axonal regeneration, we employed Gap43, the quintessential marker of axon growth, but one which can be expressed in non-regenerative situations [25], hence the caveat "putative". Upregulation of Gap43 protein in the retina was first detectable by 3d after IOP elevation. By 14 days, numerous Gap43-positive axons were observed in the pre-laminar ONH, some extending to the transition region of the ONH. For comparative purposes, we analysed Gap43 in rats subjected to NMDA-induced excitotoxicity and ON crush. After NMDA treatment, no Gap43 expression was detected, a result consistent with early RGC somal death. After ON crush, substantial Gap43 immunoreactivity was observed, which extended to the crush site. The overall results provide further evidence that the ONH is the principal site of axonal injury in this rat glaucoma model and that chronically raised IOP induces a crush-like insult at this location.

Acknowledgments The authors are grateful to the NHMRC (508123, 565202, 626964) and the Ophthalmic Research Institute of Australia for providing financial support and to Mark Daymon for expert technical assistance.

References

1. Anderson DR, Hendrickson A (1974) Effect of intraocular pressure on rapid axoplasmic transport in monkey optic nerve. Invest Ophthalmol 13:771–783
2. Balaratnasingam C, Morgan WH, Bass L, Matich G, Cringle SJ, Yu DY (2007) Axonal transport and cytoskeletal changes in the laminar regions after elevated intraocular pressure. Invest Ophthalmol Vis Sci 48:3632–3644
3. Benowitz L, Yin Y (2008) Rewiring the injured CNS: lessons from the optic nerve. Exp Neurol 209:389–398
4. Blaugrund E, Lavie V, Cohen I, Solomon A, Schreyer DJ, Schwartz M (1993) Axonal regeneration is associated with glial migration: comparison between the injured optic nerves of fish and rats. J Comp Neurol 330:105–112
5. Buckingham BP, Inman DM, Lambert W et al (2008) Progressive ganglion cell degeneration precedes neuronal loss in a mouse model of glaucoma. J Neurosci 28:2735–2744
6. Caleo M, Menna E, Chierzi S, Cenni MC, Maffei L (2000) Brain-derived neurotrophic factor is an anterograde survival factor in the rat visual system. Curr Biol 10:1155–1161
7. Casson RJ (2006) Possible role of excitotoxicity in the pathogenesis of glaucoma. Clin Exp Ophthalmol 34:54–63
8. Chauhan BC, Levatte TL, Garnier KL et al (2006) Semiquantitative optic nerve grading scheme for determining axonal loss in experimental optic neuropathy. Invest Ophthalmol Vis Sci 47:634–640
9. Chidlow G, Holman MC, Wood JP, Casson RJ (2010) Spatiotemporal characterization of optic nerve degeneration after chronic hypoperfusion in the rat. Invest Ophthalmol Vis Sci 51:1483–1497
10. Chidlow G, Osborne NN (2003) Rat retinal ganglion cell loss caused by kainate, NMDA and ischemia correlates with a reduction in mRNA and protein of Thy-1 and neurofilament light. Brain Res 963:298–306
11. Chidlow G, Wood JP, Manavis J, Osborne NN, Casson RJ (2008) Expression of osteopontin in the rat retina: effects of excitotoxic and ischemic injuries. Invest Ophthalmol Vis Sci 49:762–771
12. Crish SD, Sappington RM, Inman DM, Horner PJ, Calkins DJ (2010) Distal axonopathy with structural persistence in glaucomatous neurodegeneration. Proc Natl Acad Sci USA 107:5196–5201

13. Doster SK, Lozano AM, Aguayo AJ, Willard MB (1991) Expression of the growth-associated protein GAP-43 in adult rat retinal ganglion cells following axon injury. Neuron 6:635–647
14. Ebneter A, Casson RJ, Wood JP, Chidlow G (2010) Microglial activation in the visual pathway in experimental glaucoma: spatio-temporal characterisation and correlation with axonal injury. Invest Ophthalmol Vis Sci
15. Fujita Y, Imagawa T, Uehara M (2000) Comparative study of the lamina cribrosa and the pial septa in the vertebrate optic nerve and their relationship to the myelinated axons. Tissue Cell 32:293–301
16. Howell GR, Libby RT, Jakobs TC et al (2007) Axons of retinal ganglion cells are insulted in the optic nerve early in DBA/2J glaucoma. J Cell Biol 179:1523–1537
17. Jakobs TC, Libby RT, Ben Y, John SW, Masland RH (2005) Retinal ganglion cell degeneration is topological, but not cell type specific in DBA/2J mice. J Cell Biol 171:313–325
18. John SW (2005) Mechanistic insights into glaucoma provided by experimental genetics the Cogan lecture. Invest Ophthalmol Vis Sci 46:2649–2661
19. John SW, Smith RS, Savinova OV et al (1998) Essential iris atrophy, pigment dispersion, and glaucoma in DBA/2J mice. Invest Ophthalmol Vis Sci 39:951–962
20. Johnson EC, Deppmeier LM, Wentzien SK, Hsu I, Morrison JC (2000) Chronology of optic nerve head and retinal responses to elevated intraocular pressure. Invest Ophthalmol Vis Sci 41:431–442
21. Kalesnykas G, Niittykoski M, Rantala J et al (2007) The expression of heat shock protein 27 in retinal ganglion and glial cells in a rat glaucoma model. Neuroscience 150:692–704
22. Kashiwagi K, Ou B, Nakamura S, Tanaka Y, Suzuki M, Tsukahara S (2003) Increase in dephosphorylation of the heavy neurofilament subunit in the monkey chronic glaucoma model. Invest Ophthalmol Vis Sci 44:154–159
23. Kass MA, Heuer DK, Higginbotham EJ et al (2002) The Ocular Hypertension Treatment Study: a randomized trial determines that topical ocular hypotensive medication delays or prevents the onset of primary open-angle glaucoma. Arch Ophthalmol 120:701–713
24. Krueger Naug AM, Emsley JG, Myers TL, Currie RW, Clarke DB (2002) Injury to retinal ganglion cells induces expression of the small heat shock protein Hsp27 in the rat visual system. Neuroscience 110:653–665
25. Leon S, Yin Y, Nguyen J, Irwin N, Benowitz LI (2000) Lens injury stimulates axon regeneration in the mature rat optic nerve. J Neurosci 20:4615–4626
26. Levkovitch-Verbin H, Quigley HA, Martin KR, Valenta D, Baumrind LA, Pease ME (2002) Translimbal laser photocoagulation to the trabecular meshwork as a model of glaucoma in rats. Invest Ophthalmol Vis Sci 43:402–410
27. Livak KJ, Schmittgen TD (2001) Analysis of relative gene expression data using real-time quantitative PCR and the 2(-Delta Delta C(T)) Method. Methods 25:402–408
28. Martin KR, Quigley HA, Valenta D, Kielczewski J, Pease ME (2006) Optic nerve dynein motor protein distribution changes with intraocular pressure elevation in a rat model of glaucoma. Exp Eye Res 83:255–262
29. Minckler DS, Bunt AH, Johanson GW (1977) Orthograde and retrograde axoplasmic transport during acute ocular hypertension in the monkey. Invest Ophthalmol Vis Sci 16:426–441
30. Morin PJ, Abraham CR, Amaratunga A et al (1993) Amyloid precursor protein is synthesized by retinal ganglion cells, rapidly transported to the optic nerve plasma membrane and nerve terminals, and metabolized. J Neurochem 61:464–473
31. Morin PJ, Liu NG, Johnson RJ, Leeman SE, Fine RE (1991) Isolation and characterization of rapid transport vesicle subtypes from rabbit optic nerve. J Neurochem 56:415–427
32. Morrison J, Farrell S, Johnson E, Deppmeier L, Moore CG, Grossmann E (1995) Structure and composition of the rodent lamina cribrosa. Exp Eye Res 60:127–135
33. Morrison JC, Johnson EC, Cepurna W, Jia L (2005) Understanding mechanisms of pressure-induced optic nerve damage. Prog Retin Eye Res 24:217–240
34. Pant HC (1988) Dephosphorylation of neurofilament proteins enhances their susceptibility to degradation by calpain. Biochem J 256:665–668
35. Petzold A (2005) Neurofilament phosphoforms: surrogate markers for axonal injury, degeneration and loss. J Neurol Sci 233:183–198
36. Pfaffl MW (2001) A new mathematical model for relative quantification in real-time RT-PCR. Nucleic Acids Res 29:e45
37. Quigley H, Anderson DR (1976) The dynamics and location of axonal transport blockade by acute intraocular pressure elevation in primate optic nerve. Invest Ophthalmol 15:606–616
38. Quigley HA, Addicks EM (1980) Chronic experimental glaucoma in primates. II. Effect of extended intraocular pressure elevation on optic nerve head and axonal transport. Invest Ophthalmol Vis Sci 19:137–152
39. Quigley HA, Addicks EM, Green WR, Maumenee AE (1981) Optic nerve damage in human glaucoma. II. The site of injury and susceptibility to damage. Arch Ophthalmol 99:635–649
40. Quigley HA, Anderson DR (1977) Distribution of axonal transport blockade by acute intraocular pressure elevation in the primate optic nerve head. Invest Ophthalmol Vis Sci 16:640–644
41. Ruifrok AC, Johnston DA (2001) Quantification of histochemical staining by color deconvolution. Anal Quant Cytol Histol 23:291–299
42. Salinas-Navarro M, Alarcon-Martinez L, Valiente-Soriano FJ et al (2010) Ocular hypertension impairs optic nerve axonal transport leading to progressive retinal ganglion cell degeneration. Exp Eye Res 90:168–183
43. Schlamp CL, Johnson EC, Li Y, Morrison JC, Nickells RW (2001) Changes in Thy1 gene expression associated with damaged retinal ganglion cells. Mol Vis 7:192–201
44. Schlamp CL, Li Y, Dietz JA, Janssen KT, Nickells RW (2006) Progressive ganglion cell loss and optic nerve degeneration in DBA/2J mice is variable and asymmetric. BMC Neurosci 7:66
45. Soto I, Oglesby E, Buckingham BP et al (2008) Retinal ganglion cells downregulate gene expression and lose their axons within the optic nerve head in a mouse glaucoma model. J Neurosci 28:548–561